

Optimization of the ultrasonic treatment for Tara gum using response surface methodology

Barbara da Silva Soares¹ , Carlos Wanderlei Piler de Carvalho² , Edwin Elard Garcia-Rojas^{1,3*} 

¹Programa de Pós-graduação em Ciência e Tecnologia de Alimentos – PPGCTA, Universidade Federal Rural de Rio de Janeiro – UFRRJ, Seropédica, RJ, Brasil

²Laboratório de Análises Físicas de Alimentos, Embrapa Agroindústria de Alimentos, Guaratiba, RJ, Brasil

³Departamento de Engenharia de Agronegócios – VEA, Universidade Federal Fluminense – UFF, Volta Redonda, RJ, Brasil

*edwinr@id.uff.br

Abstract

High-intensity ultrasound irradiation proved to be an effective method for modifying tara gum by generating low molecular weight products and better water solubility. The objectives of this research were to optimize the parameters for the high-intensity ultrasonic treatment with response surface methodology and improve the tara gum solubility. The results demonstrated that after the ultrasound treatment, the solubility of the tara gum had increased (17.7%) as a result of the reduced intrinsic viscosity (70%). The molecular weight of the untreated tara gum was 1.89×10^6 Da, and after ultrasound treatment, it was reduced to 0.47×10^6 Da. Rheological analyses confirmed the reduction in molecular weight for the modified and optimized tara gum and the resulting increase in solubility. This knowledge provides a better understanding of ultrasound treatment technology and increases the scope for use of tara gum in the food industry.

Keywords: *depolymerization, galactomannan, solubility, sonication, viscosity.*

How to cite: Soares, B. S., Carvalho, C. W. P., & Garcia-Rojas, E. E. (2023). Optimization of the ultrasonic treatment for Tara gum using response surface methodology. *Polímeros: Ciência e Tecnologia*, 33(1), e20230003. <https://doi.org/10.1590/0104-1428.20220090>

1. Introduction

Tara gum (TG), also called Peruvian carob, is a polymer obtained by grinding the endosperm of *Caesalpinia spinosa* tree seeds. Peru is the largest producer of TG, with approximately 80% of the total cultivation. TG is a galactomannan with functionality and structure similar to those of guar and carob gums; however, the mannose/galactose ratios differ, and they are 3/1 for TG, 2/1 for guar gum and 4/1 for carob gum^[1]. Due to its similar functional properties, TG has been considered an important alternative with which to relieve the short supply of the two common galactomannan sources (guar gum and carob gum)^[2], and it exhibits other advantages, such as easy availability, nontoxicity, biocompatibility and biodegradability^[2]. Galactomannans are neutral hydrophilic polysaccharides with approximate molecular weights (Mw) of 1.0×10^6 g·mol⁻¹, and they contain a linear chain of (1-4)- β -D-mannopyranoses linked to α -D-galactopyranosyl units via (1-6) glycosidic bonds^[3]. The galactomannan from TG has a high molecular weight, and like other polysaccharides, its chemical structure, monosaccharide composition, bonding modes and branched structures can compromise the biological activities of the polysaccharide^[4]. Various studies have reported that high molecular weight polysaccharides exhibit high viscosity and low solubility in water, which could reduce their biological activity and possibly limit application of the polysaccharides^[4-6]. Aqueous

TG solutions are neutral and highly viscous^[6]. To dissolve TG completely, heating is necessary, which can be considered a disadvantage in economic and practical terms.

In this context, high-intensity ultrasound (HIUS) with frequencies between 20-100 kHz and intensities above 1 W/cm² proved to be effective in depolymerization and generation of products exhibiting low molecular weight and better solubility in water^[7,8], and it is a green technology; it does not require or produce unwanted chemical products (that is, it does not produce substances that could contaminate the final product), which allows broader application in the pharmaceutical, cosmetic and the food industries. HIUS is widely used to improve the functionality and change the structures of proteins^[9], as in the ultrasound-assisted extraction of new galactomannans and polysaccharides^[10] and in modification of various galactomannans and polysaccharides, including pectin^[11,12], sodium alginate^[13], konjac glucomannan^[6] and TG recently studied in our laboratory^[14]. Thus, the use of a simple sonication method for reducing and increasing the solubilities of polysaccharides represents an important adaptation of the mechanical properties of TG solutions, enabling more adequate and rational uses of the polysaccharides in various fields. However, these previous studies have only superficially addressed the effects of ultrasound, and the ultrasonic parameters have not been optimized. Furthermore,

the effects of HIUS on galactomannans, especially those in tara gum, have been sparsely reported.

In this study, the parameters such as time, amplitude and concentration were optimized by means of response surface methodology after treatment of aqueous solutions of TG with HIUS, and the effects of HIUS on the physicochemical and rheological properties of the TG were evaluated.

2. Materials and Methods

2.1 Materials

Tara gum (TG, purity $\geq 90\%$) was obtained from Silvateam Peru (Lima, Peru). Ultra-pure water with a conductivity of $0.05 \mu\text{S}/\text{cm}$ was obtained from Gehaka Master-P&D (São Paulo, Brazil).

2.2 Experimental design

In using the response surface methodology (RSM), three independent variables were considered: X_1 is the sonication time (2.84 to 112.15 min), X_2 is the TG concentration (0.19 to 1.20% w/v) and X_3 is the amplitude (26 to 93%), and the dependent variable is the intrinsic viscosity (Y). A control was prepared without the ultrasound treatment. The methodology used was as described by Li et al.^[15]. The quadratic polynomial regression model (Equation 1) was employed to correlate these values to their coded variables:

$$Y = b_0 + b_1X_1 + b_2X_2 + b_3X_3 + b_{11}X_1^2 + b_{22}X_2^2 + b_{33}X_3^2 + b_{12}X_1X_2 + b_{13}X_1X_3 + b_{23}X_2X_3 \quad (1)$$

Where b_0 (constant term); b_1 , b_2 and b_3 (linear effects); b_{11} , b_{22} and b_{33} (quadratic effects); and b_{12} , b_{13} and b_{23} (interaction effects) represent the coefficients of the polynomial model.

A software package (SAS® 9.0 ADX Interface for Design of Experiments) was used for analyses of the experimental data. The optimal condition for each variable was obtained by applying the numerical optimization procedure.

2.3 Ultrasonic treatment

Solutions of TG with the desired concentrations (0.19 to 1.20% w/v) were prepared with ultrapure water and stirred at 300 rpm (SP-160, SP Labor, Brazil) overnight at room temperature (25 °C). Then, the dispersion was transferred to a jacketed beaker connected in a thermoregulated bath with external circulation (Quimis, Q214M2, Brazil) at $25 \text{ °C} \pm 0.01$ and stirred with a C-MAG HS 7 magnetic stirrer (IKA, Staufen, Germany) at 200 rpm throughout the process. The samples were subjected to HIUS by employing an ultrasound generator (UP 100H, Hielschier, Germany) containing a titanium sonotrode (MS2, 2 mm diameter); the frequency was 30 kHz and the power was 100 W. The ultrasound probe was submerged in the sample to a depth of 0.5 cm.

2.4 Determination of intrinsic viscosities

The intrinsic viscosities were measured with the method of Li et al.^[15]. The relative viscosities (η_r) of the untreated tara gum (UTG) and tara gum-treated and optimized (TGTO) samples were measured with capillary viscometers

(Schott-Gerate, Germany), and the capillaries were immersed in a thermostatic bath (CT-52, Schott-Gerate, Germany) at $25 \text{ °C} \pm 0.05$. The intrinsic viscosities $[\eta]$ were calculated with Equations 2 and 3:

$$\eta_r = \frac{t_s}{t_0}, \eta_{sp} = \eta_r - 1 \quad (2)$$

$$[\eta] = \frac{\sqrt{2\eta_{sp} - \ln \eta_r}}{c} \quad (3)$$

where t_s is the flow time of the solution with UTG and TGTO, t_0 is the flow time of the solvent, η_r is the relative viscosity, η_{sp} is the incremental viscosity, and c is the concentration of UTG and TGTO (g/mL).

2.5 Physicochemical characterization of UTG and TGTO

2.5.1 Molecular weight

The molecular weights of UTG and TGTO were determined with an adapted viscosimetric method^[16]. In summary, the dynamic viscosity was calculated with data obtained from Cannon-Fenske capillary viscometers (Schott-Gerate, Germany), in which aqueous solutions containing UTG and TGTO were prepared at concentrations from 0.01 to 0.05%. The sample readings were taken in triplicate. The intrinsic viscosity was estimated by extrapolation of Martin's curves to "zero" concentration using Equations 4 and 5:

$$\ln(\eta_{sp}/c) = \ln[\eta] + K[\eta]c \quad (4)$$

$$\eta_{sp} = \frac{\eta - \eta_0}{\eta} \quad (5)$$

where $[\eta]$ is the intrinsic viscosity (cm^3/g), η_{sp} is the specific viscosity, c is the concentration of the TG (g/mL), η is the solution viscosity of the TG (g/cm.s), η_0 is the solvent viscosity (g/cm.s), and K is Martin's constant.

The molecular weight was estimated with the Mark-Houwink Equation 6:

$$[\eta] = 11.55 \times 10^{-6} [(1-\alpha)\bar{M}_v]^{0.98} \quad (6)$$

where $[\eta]$ is the intrinsic viscosity (dL/g), \bar{M}_v is the average viscosimetric molecular weight expressed as g mol^{-1} and α is a constant related to the structure of galactomannan, which was determined with Equation 7:

$$\alpha = 1 / [(M/G) + 1] \quad (7)$$

where the mannose:galactose (M:G) ratio is the ratio of mannose and galactose in the polysaccharide structure, which was obtained from nuclear magnetic resonance spectroscopy ($^1\text{H NMR}$). The decrease in $[\eta]$ is equivalent to the decrease in the average molecular mass, so it can be considered an indication of TG degradation before and after ultrasound treatment and optimization.

2.5.2 Average particle size determination

The hydrodynamic diameters (d.nm) of the 0.1% (w/v) UTG and TGTO solutions were determined using a Zetasizer

(Malvern Instruments, Nano-ZS, UK) at 632.8 nm with a 90° angle at 25 °C, and the experiments were performed in triplicate.

2.5.3 Fourier Transform Infrared (FTIR) Spectra of UTG and TGTO

The spectra were determined with an FTIR spectrometer (Bruker, Vertex 70, Germany) over the range 4000–500 cm⁻¹.

2.6 Solubility of UTG and TGTO

Solubilities were determined according to the method of Rodriguez-Canto et al.^[17]. Freeze-dried samples were prepared at 0.1% (w/v) in distilled water and stirred with a magnetic stirrer (C-MAG HS 7, IKA, Germany) at room temperature (25 °C) for 1 h. The samples were centrifuged (Digicen 21R, OrtoAlresa, Spain) at 3500 × g for 30 min at 25 °C to remove the insoluble material. Then, the supernatant was collected and dried in an oven (SX 1.3, Sterilifer, Brazil) at 105 °C for 24 h.

2.7 Rheological analyses of the UTG and TGTO solutions

2.7.1 Measurements of constant shear

All rheological properties, including the flow behavior with increasing shear rate and frequency sweep tests of the UTG and TGTO, were measured at a constant temperature of 25 °C with a MARS II rotational rheometer (Thermo Fisher Scientific, Karlsruhe, Germany) equipped with a plate-and-plate geometry (PP 60Ti, 60 mm diameter). The UTG and TGTO solutions were prepared in deionized water with concentrations of 1.0%, 3.0% and 4.0% (w/v), and constant shear rate tests were performed over the range 0.01 to 300 s⁻¹ at 25 °C. The flow behavior was analyzed with the rheological models of Newton (Equation 8), the power law (Equation 9), Bingham (Equation 10) and Herschel-Bulkley (Equation 11):

$$\tau = \eta \cdot \dot{\gamma} \quad (8)$$

$$\tau = K \cdot (\dot{\gamma})^n \quad (9)$$

$$\tau - \tau_0 = \eta_{pl} \cdot \dot{\gamma} \quad (10)$$

$$\tau - \tau_0 = K \cdot (\dot{\gamma})^n \quad (11)$$

where τ is the shear stress (Pa), $\dot{\gamma}$ is the shear rate (s⁻¹), η is the Newtonian viscosity (Pa · s), K is the consistency coefficient Pa · sⁿ, n is the flow behavior index (dimensionless), τ_0 is the initial yield stress (Pa), and η_{pl} is the Bingham plastic viscosity (Pa · s). The quality of the fit was evaluated from the coefficient of determination (R²).

2.7.2 Dynamic shear measurements

Dynamic oscillatory measurements were performed to ensure linear viscoelastic conditions with frequency sweep tests performed over the range 0.1 to 100 Hz for UTG and TGTO (1%) and over the range 0.1 to 10 Hz for TGTO (3% and 4%) by applying a constant shear stress for analyses of the storage modulus (G') and loss modulus (G'') as a function of the oscillation frequency.

2.8 Statistical analyses

One-way analysis of variance (ANOVA) and Tukey's test were used to establish the significance of differences between mean values at the 0.05 significance level. The statistical analyses were performed with Origin® 8.5 software (OriginLab Corporation, USA).

3. Results and Discussion

3.1 Optimization of the experimental design

The effects of different HIUS treatments on the intrinsic viscosity are presented in Table S1, and the regression analysis and ANOVA are presented in Table S2. This table shows that only the linear model was significant (p < 0.05), and the value of the coefficient of determination (R²) was 79.39, suggesting that the regression equation obtained with the RSM was viable. The analysis suggested that the linear effects of the time and concentration variables were significant (p < 0.05), and there was no significant effect (p < 0.05) for the amplitude variable. Using the linear model, the decoded Equation 12 was developed for the intrinsic viscosity:

$$\eta = 12.14 - 2.11 \cdot t + 1.25 \cdot C \quad (12)$$

where η is the intrinsic viscosity, t is the time and C is the gum concentration. Based on the predicted model, the optimal conditions for the experiment in which the variables were tested included a time of 112 min, a concentration of 0.19% (w/v) and an amplitude of 60%.

With these optimized conditions, the intrinsic viscosity was 5.97 (dL/g) according to the SAS program. This result was attributed to the greater exposure (112 min) of the TG to the HIUS, which increased the number of cavitation events, generated free radicals, enabled depolymerization of the TG and, consequently, generated TG with a low intrinsic viscosity^[15,18]. These results agreed with the response surface plot shown in Figure 1.

3.2 Effects of the ultrasonic treatment on the physicochemical properties of UTG and TGTO.

3.2.1 Intrinsic viscosity, molecular weight and particle size

The ultrasonic treatments caused substantial decreases in the intrinsic viscosity of TG due to reductions in the molecular weight and chain length of the gum. The intrinsic viscosities of UTG and TGTO were 12.31 dL/g and 3.14 dL/g, respectively. The degradation rate of TG was estimated to be 59%. The average molecular weight (Mw) was higher for UTG (1.89 × 10⁶ Da) than for TGTO (0.47 × 10⁶ Da), which was consistent with the reductions in the intrinsic viscosity, indicating that ultrasound was an effective method for TG depolymerization. The average hydrodynamic diameter (Z-average) of UTG was 147.1 ± 4.90 nm, while that of TGTO was 139.7 ± 2.4 nm. Figure 2 shows the distributions of the UTG and TGTO particle sizes. For UTG (Figure 2A), we observed that the size distribution was wide and contained 3 uneven peaks, whereas TGTO (Figure 2B) showed 2 narrower and more uniform peaks.

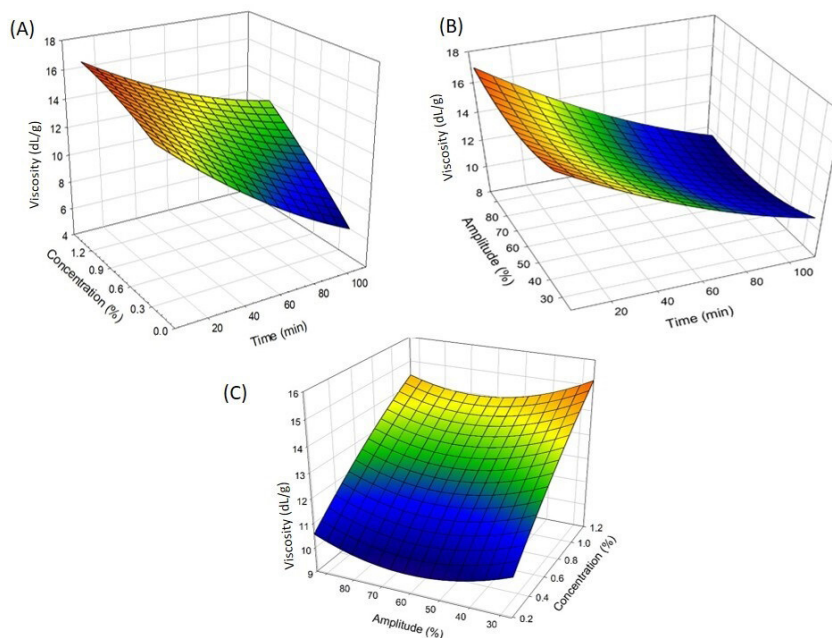


Figure 1. Influence of treatment parameters on the viscosity. Effects of time and concentration (A), time and amplitude (B) and concentration and amplitude (C) on the intrinsic viscosity of the TG.

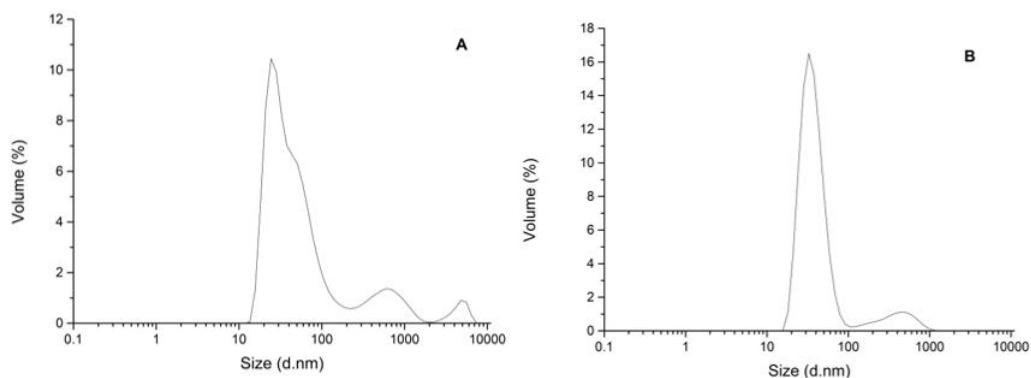


Figure 2. Particle size distributions of UTG (A) and TGTO (B).

The reductions and uniformity of the particle sizes observed in this study may have been related to cavitation in the aqueous TG solution caused by the HIUS treatment. According to Li et al.^[15], shear forces alter the structures of polysaccharides after explosion of the cavitation bubbles generated by the ultrasonic treatment, disperse the polysaccharide aggregates and cause reductions in the molecular weights and particle sizes. Our results agree with other studies in which polysaccharides were degraded with ultrasonic irradiation^[4,6].

3.2.2 Analysis of the FTIR spectra

Figure 3 shows that both UTG and TGTO showed broad absorption bands at 3319 and 3368 cm^{-1} , respectively. These could be due to hydrogen bonding involving the hydroxyl groups in the gum molecules and correspond to O-H

stretching vibrations. The band at 2918 cm^{-1} was attributed to symmetric CH stretching vibrations^[14,19]. The absorption band at approximately 1638 cm^{-1} corresponded to the asymmetric stretching vibrations of C-O bonds^[4]. The peaks at 1023 cm^{-1} for TGTO and 1014 cm^{-1} for UTG indicated bending vibrations of $\text{H}_2\text{C-O-CH}_2$ bonds^[14,19]. The spectra of UTG and TGTO showed absorption bands at 810 cm^{-1} characteristic of α -linked D-galactopyranose units, and at 871 cm^{-1} characteristic of β -linked D-mannopyranose. The infrared spectra of UTG and TGTO clearly showed that there were no major changes in the functional groups or chemical structures caused by the treatments and that ultrasound-induced chain scissions only broke the polymer structures and resulted in viscosity reductions without any changes in the primary structures

or in the functional properties of the tara gum, as reported previously^[4,6,12].

3.3. Effects of ultrasound on the solubilities of UTG and TGTO

The solubilities of TGTO and UTG were 99.67 and 84.67%, respectively. TGTO showed a more significant increase in the water solubility, approximately 17.5%, compared to UTG. The ultrasonic waves caused cavitation due to the expansion and contraction cycles experienced by the material, and these cycles disrupted the cell walls of the solid matrix^[20]. These ruptures enabled solvent penetration, which explains the increase seen in the TG solubility after the ultrasound treatment. Furthermore, this result may be related to destruction of intra- and intermolecular noncovalent bonds, which would expose more hydrophilic polysaccharide groups to water and increase the solubility^[21]. The current study achieved a better result than the study carried out by Santos, Isabel and Garcia-Rojas^[14], in which the solubility of TG was 83% after sonication for 60 min at 25 °C. The higher solubility found in this study is consistent with the results described above (Item 3.2.1), in which prolonged exposure to sonication contributed to a greater reduction in the molecular weight and, consequently, an increase in the solubility. Ultrasound-induced increases in the solubilities of polysaccharides have already been reported^[21], but studies with galactomannans are still scarce.

The development of new technologically sophisticated products via nonthermal processing is one of the major trends for the coming years^[22]. In this sense, it should be noted that the solubility achieved in this research was possible only with application of the optimized ultrasonic treatment method, and prior thermal processing was not required. There is

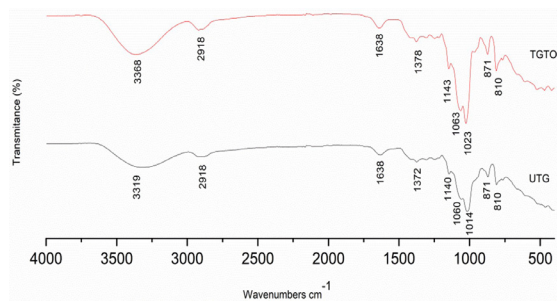


Figure 3. FTIR spectra of UTG (untreated) and TGTO (after optimized treatment).

global demand for new products similar to unprocessed and made with nonthermal technologies. Thus, the food industry could apply an adapted form of TGTO^[23]. Consumers are demanding foods with innovative ingredients, and in the future, TGTO can be used to prepare functional foods and beverages from ingredients that are easily soluble at room temperature, such as with instant foods. In addition, the modified TGTO can be used in packages with edible films that require a material with low water resistance that is biodegradable and safe for human consumption.

3.4 Rheological Properties of the UTG and TGTO

Table 1 summarizes the parameters of the Newtonian, power law, Bingham and Herschel-Bulkley models obtained by fitting the rheological data of the UTG (1%, w/v) and TGTO (1, 3 and 4%, w/v) solutions. Thus, the flow behaviors of the UTG and TGTO solutions were best described by the power law model, which presented R^2 values close to 1 ($R^2= 0.99$ and 0.97). An increase in the concentration of TGTO from 1 to 4% resulted in an increase in the consistency coefficient K and a decrease in the flow behavior index n (Table 1). This indicated that the solutions became more resistant to flow and were increasingly pseudoplastic as the concentration of TGTO was increased. According to Wei et al.^[24], gums with low n values and improved pseudoplasticities are advantageous because they provide a less viscous mouthfeel with easier mixing and serve as thickeners in nutritional formulations used for the management of dysphagia. When comparing UTG and TGTO, we observed a reduction in the consistency coefficient K from 6.806 ± 1.336 to 0.029 ± 0.001 at a 1% concentration. The modifications in the rheological properties are useful, as they confirm a reduction in the molecular weight of TG and consequently the increased solubility.

The flow and apparent viscosity curves of UTG and TGTO are shown in Figure 4A and B. Non-Newtonian behavior was observed for the UTG with decreasing viscosity and increasing strain rate. The TGTO presented as a Newtonian fluid with a very low viscosity close to that of water. This behavior was attributed to breaking of the polymeric network and orientation or alignment of the microstructures along the direction of shear flow, which reduced the flow resistance^[25]. This indicated that the ultrasound treatment caused strong changes in the rheological properties due to a reduction of the molecular mass of the TGTO and was consistent with other studies that treated polysaccharides with ultrasound^[6,13].

Table 1. Rheological parameters obtained from the Newton, Power Law, Bingham, and Herschel-Bulkley models for UTG and TGTO solutions at 25 °C.

Sample	Newton		Power law			Bingham			Herschel-Bulkley			
	η	R^2	K	n	R^2	τ_0	η_{pl}	R^2	K	N	τ_0	R^2
UGT (1%)	0.28	0.41	6.80	0.40	0.99	24.2	0.16	0.94	23.1	0.25	-26.8	0.99
TGTO (1%)	0.02	0.97	0.02	0.90	0.97	0.1	0.02	0.97	0.04	0.84	-0.16	0.97
TGTO (3%)	0.48	0.99	0.98	0.86	0.99	6.5	0.45	0.99	1.10	0.84	-1.74	0.99
TGTO (4%)	1.21	0.98	3.67	0.79	0.99	26.3	1.08	0.99	5.26	0.73	-12.8	0.99

where τ is the shear stress (Pa), $\dot{\gamma}$ is the shear rate (s^{-1}), η is the Newtonian viscosity (mPa·s), K is the consistency coefficiente $Pa \cdot s^{-n}$, n is the flow behavior index (dimensionless), τ_0 is the initial yield stress (Pa), η_{pl} is the Bingham plastic viscosity (Pa·s) and coefficient of determination (R^2).

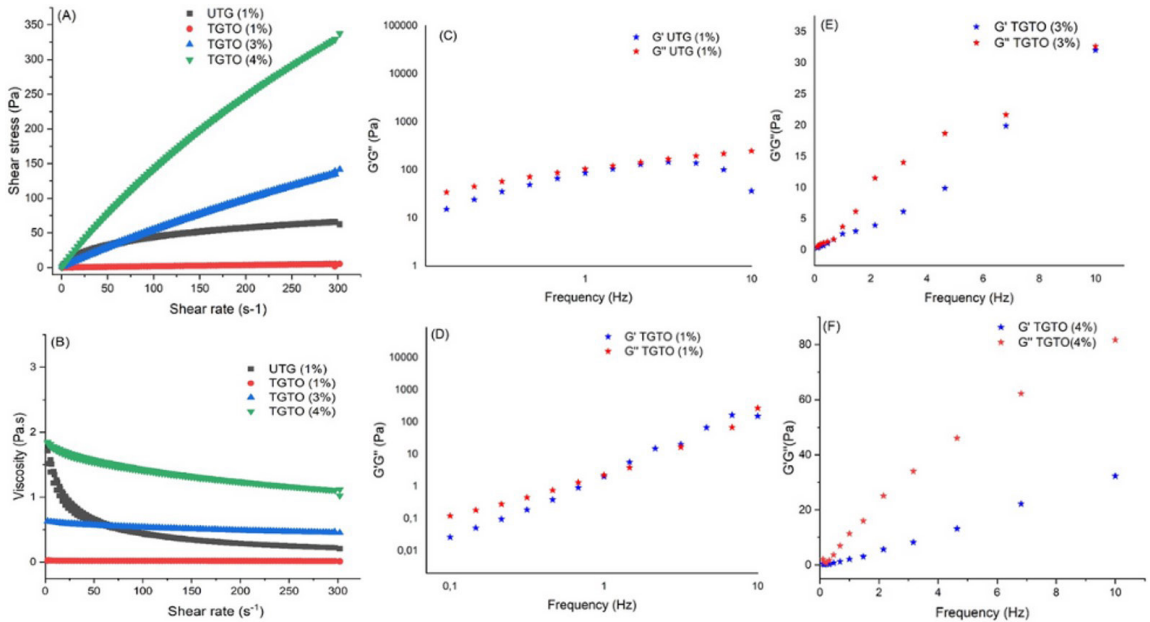


Figure 4. Rheological measurements of the UTG and TGTO solutions. Flow curves (A), apparent viscosity curves for the UTG and TGTO solutions (B); storage and loss moduli (G' , G'') for UTG at a 1% concentration (C) and TGTO at a 1% concentration (D) and at 3% (E) and 4% (F) at 25 °C.

The plots of G' and G'' as a function of frequency for the UTG solution presented crossover points ($G' = G''$) at low frequencies (1 to 10 Hz). Initially, the solutions behaved as liquids with G'' higher than G' , and after the crossing point, elastic behavior was established with G' higher than G'' Figure 4C and D, as found in other studies^[6,16]. At frequencies above 10 Hz, G' and G'' showed nonlinearity corresponding to disentanglement and irreversible flow of the UTG and TGTO molecules as a result of the shear force^[6]. In Figure 4E and F, in which TGTO has higher concentrations of 3% and 4%, the solutions behaved as liquids with G'' higher than G' . Furthermore, both the G' and G'' for TGTO decreased, possibly due to breaking of the polymer chain^[6]. In water, the UTG formed a relatively elastic dispersion (solid property) that became a viscous dispersion (fluid property) after ultrasound treatment. These results corroborated the results of Li et al.^[6], who studied the ultrasonic degradation and rheological profiles of konjac glucomannan (KGM) and observed that ultrasound weakened the intermolecular interactions.

4. Conclusion

A high-intensity ultrasound treatment significantly affected the physicochemical, functional, and rheological properties of TG, depending on the ultrasound treatment time and polymer concentration. After the ultrasound treatment, the TG showed a reduction in the intrinsic viscosity and particle sizes. These changes positively influenced the functional properties of the TG, as shown by the increased solubility. In addition, the TGTO solution behaved as a Newtonian fluid with low viscosity and consistency; this indicated that the ultrasound treatment caused strong changes in the

rheological properties of the TG solution and confirmed the effectiveness of the treatment. The increased solubility of galactomannan, the reduced viscosity, and the reduction in molecular mass, will enable future technological applications, such as with functional beverages, instant foods and edible film packaging. In addition to biological applications involving the antioxidant activity and bioaccessibility of TG, it meets the various demands of the food processing industry. Therefore, advances in ultrasonication treatments of natural polymers are expected to provide new applications in various industrial fields.

5. Author's Contribution

- **Conceptualization** – Barbara da Silva Soares; Edwin Elard Garcia-Rojas.
- **Data curation** – Barbara da Silva Soares.
- **Formal analysis** – Barbara da Silva Soares.
- **Funding acquisition** – Edwin Elard Garcia-Rojas.
- **Investigation** – Barbara da Silva Soares.
- **Methodology** – Barbara da Silva Soares; Carlos Wanderlei Piler Carvalho; Edwin Elard Garcia-Rojas.
- **Project administration** – Edwin Elard Garcia-Rojas.
- **Resources** – Carlos Wanderlei Piler Carvalho; Edwin Elard Garcia-Rojas.
- **Software** – NA.
- **Supervision** – Edwin Elard Garcia-Rojas.
- **Validation** – Barbara da Silva Soares; Carlos Wanderlei Piler Carvalho; Edwin Elard Garcia-Rojas.
- **Visualization** – NA.

- **Writing – original draft** – Barbara da Silva Soares.
- **Writing – review & editing** – Barbara da Silva Soares; Carlos Wanderlei Piler Carvalho; Edwin Elard Garcia-Rojas.

6. Acknowledgements

The authors thank Conselho Nacional de Desenvolvimento Científico e Tecnológico, Brazil (313928/2021-5); Coordenação de Aperfeiçoamento de Pessoal de Nível Superior, Brazil (Code 001), and Fundação de Amparo à Pesquisa do Estado do Rio de Janeiro, Brazil (E-26/201.030/2021) for financial support

7. References

1. Wu, Y., Ding, W., Jia, L., & He, Q. (2015). The rheological properties of tara gum (*Caesalpinia spinosa*). *Food Chemistry*, *168*, 366-371. <http://dx.doi.org/10.1016/j.foodchem.2014.07.083>. PMID:25172722.
2. Wu, Y., Ding, W., & He, Q. (2016). Molecular characteristics of tara galactomannans: effect of degradation with hydrogen peroxide. *International Journal of Food Properties*, *20*(12), 3014-3022. <http://dx.doi.org/10.1080/10942912.2016.1270300>.
3. Martin, A. A., Sasaki, G. L., & Sierakowski, M. R. (2020). Effect of adding galactomannans on some physical and chemical properties of hyaluronic acid. *International Journal of Biological Macromolecules*, *144*, 527-535. <http://dx.doi.org/10.1016/j.ijbiomac.2019.12.114>. PMID:31857166.
4. Xu, Y., Zhang, X., Yan, X.-H., Zhang, J.-L., Wang, L.-Y., Xue, H., Jiang, G.-C., Ma, X.-T., & Liu, X.-J. (2019). Characterization, hypolipidemic and antioxidant activities of degraded polysaccharides from *Ganoderma lucidum*. *International Journal of Biological Macromolecules*, *135*, 706-716. <http://dx.doi.org/10.1016/j.ijbiomac.2019.05.166>. PMID:31129213.
5. Chen, X., Qi, Y., Zhu, C., & Wang, Q. (2019). Effect of ultrasound on the properties and antioxidant activity of hawthorn pectin. *International Journal of Biological Macromolecules*, *131*, 273-281. <http://dx.doi.org/10.1016/j.ijbiomac.2019.03.077>. PMID:30876895.
6. Li, J., Li, B., Geng, P., Song, A.-X., & Wu, J.-Y. (2017). Ultrasonic degradation kinetics and rheological profiles of a food polysaccharide (*konjac glucomannan*) in water. *Food Hydrocolloids*, *70*, 14-19. <http://dx.doi.org/10.1016/j.foodhyd.2017.03.022>.
7. Zou, P., Lu, X., Jing, C., Yuan, Y., Lu, Y., Zhang, C., Meng, L., Zhao, H., & Li, Y. (2018). Low-molecular-weight polysaccharides from *Pyropia yezoensis* enhance tolerance of wheat seedlings (*Triticum aestivum L.*) to salt stress. *Frontiers in Plant Science*, *9*, 427. <http://dx.doi.org/10.3389/fpls.2018.00427>. PMID:29719543.
8. Tecson, M. G., Abad, L. V., Ebajo, V. D., Jr., & Camacho, D. H. (2021). Ultrasound-assisted depolymerization of kappa-carrageenan and characterization of degradation product. *Ultrasonics Sonochemistry*, *73*, 105540. <http://dx.doi.org/10.1016/j.ultsonch.2021.105540>. PMID:33812249.
9. Stefanović, A. B., Jovanović, J. R., Dojčinović, M. B., Lević, S. M., Nedović, V. A., Bugarški, B. M., & Knežević-Jugović, Z. D. (2017). Effect of the controlled high-intensity ultrasound on improving functionality and structural changes of egg white proteins. *Food and Bioprocess Technology*, *10*(7), 1224-1239. <http://dx.doi.org/10.1007/s11947-017-1884-5>.
10. Niknam, R., Mousavi, M., & Kiani, H. (2020). New studies on the galactomannan extracted from *Trigonella foenum-graecum* (Fenugreek) seed: effect of subsequent use of ultrasound and microwave on the physicochemical and rheological properties. *Food and Bioprocess Technology*, *13*(5), 882-900. <http://dx.doi.org/10.1007/s11947-020-02437-6>.
11. Zheng, J., Zeng, R., Kan, J., & Zhang, F. (2018). Effects of ultrasonic treatment on gel rheological properties and gel formation of high-methoxyl pectin. *Journal of Food Engineering*, *231*, 83-90. <http://dx.doi.org/10.1016/j.jfoodeng.2018.03.009>.
12. Chen, T.-T., Zhang, Z.-H., Wang, Z.-W., Chen, Z.-L., Ma, H., & Yan, J.-K. (2021). Effects of ultrasound modification at different frequency modes on physicochemical, structural, functional, and biological properties of citrus pectin. *Food Hydrocolloids*, *113*, 106484. <http://dx.doi.org/10.1016/j.foodhyd.2020.106484>.
13. Doderò, A., Vicini, S., & Castellano, M. (2020). Depolymerization of sodium alginate in saline solutions via ultrasonic treatments: a rheological characterization. *Food Hydrocolloids*, *109*, 106128. <http://dx.doi.org/10.1016/j.foodhyd.2020.106128>.
14. Santos, M. B., Isabel, I. C. A., & Garcia-Rojas, E. E. (2022). Ultrasonic depolymerization of aqueous tara gum solutions: kinetic, thermodynamic and physicochemical properties. *Journal of the Science of Food and Agriculture*, *102*(11), 4640-4646. <http://dx.doi.org/10.1002/jsfa.11824>. PMID:35174497.
15. Li, M., Ma, F., Li, R., Ren, G., Yan, D., Zhang, H., Zhu, X., Wu, R., & Wu, J. (2020). Degradation of *Tremella fuciformis* polysaccharide by a combined ultrasound and hydrogen peroxide treatment: process parameters, structural characteristics, and antioxidant activities. *International Journal of Biological Macromolecules*, *160*, 979-990. <http://dx.doi.org/10.1016/j.ijbiomac.2020.05.216>. PMID:32473217.
16. Fernandes, R. A., & Garcia-Rojas, E. E. (2021). Effect of cosolutes on the rheological and thermal properties of Tara gum aqueous solutions. *Journal of Food Science and Technology*, *58*(7), 2773-2782. <http://dx.doi.org/10.1007/s13197-020-04785-9>. PMID:34194111.
17. Rodríguez-Canto, W., Chel-Guerrero, L., Fernandez, V. V. A., & Aguilar-Vega, M. (2019). *Delonix regia* galactomannan hydrolysates: rheological behavior and physicochemical characterization. *Carbohydrate Polymers*, *206*, 573-582. <http://dx.doi.org/10.1016/j.carbpol.2018.11.028>. PMID:30553360.
18. Yan, J.-K., Wang, Y.-Y., Ma, H.-L., & Wang, Z.-B. (2016). Ultrasonic effects on the degradation kinetics, preliminary characterization and antioxidant activities of polysaccharides from *Phellinus linteus* mycelia. *Ultrasonics Sonochemistry*, *29*, 251-257. <http://dx.doi.org/10.1016/j.ultsonch.2015.10.005>. PMID:26585005.
19. Santos, M. B., Dos Santos, C. H. C., de Carvalho, M. G., de Carvalho, C. W. P., & Garcia-Rojas, E. E. (2019). Physicochemical, thermal and rheological properties of synthesized carboxymethyl tara gum (*Caesalpinia spinosa*). *International Journal of Biological Macromolecules*, *134*, 595-603. <http://dx.doi.org/10.1016/j.ijbiomac.2019.05.025>. PMID:31071404.
20. Wang, C.-Y. (2020). A review on the potential reuse of functional polysaccharides extracted from the by-products of mushroom processing. *Food and Bioprocess Technology*, *13*(2), 217-228. <http://dx.doi.org/10.1007/s11947-020-02403-2>.
21. Wang, W., Chen, W., Zou, M., Lv, R., Wang, D., Hou, F., Feng, H., Ma, X., Zhong, J., Ding, T., Ye, X., & Liu, D. (2018). Applications of power ultrasound in oriented modification and degradation of pectin: A review. *Journal of Food Engineering*, *234*, 98-107. <http://dx.doi.org/10.1016/j.jfoodeng.2018.04.016>.

22. Strieder, M. M., Silva, E. K., & Meireles, M. A. A. (2021). Advances and innovations associated with the use of acoustic energy in food processing: an updated review. *Innovative Food Science & Emerging Technologies*, 74, 102863. <http://dx.doi.org/10.1016/j.ifset.2021.102863>.
23. Mukherjee, K., Dutta, P., Badwaik, H. R., Saha, A., Das, A., & Giri, T. K. (2022). Food Industry applications of Tara Gum and its modified forms. *Food Hydrocolloids for Health*, 3, 100107. <http://dx.doi.org/10.1016/j.fhfh.2022.100107>.
24. Wei, Y., Guo, Y., Li, R., Ma, A., & Zhang, H. (2020). Rheological characterization of polysaccharide thickeners oriented for dysphagia management: carboxymethylated curdlan, konjac glucomannan and their mixtures compared to xanthan gum. *Food Hydrocolloids*, 110, 106198. <http://dx.doi.org/10.1016/j.foodhyd.2020.106198>.
25. Mezger, T. G. (2006). *The rheology handbook: for users of rotational and oscillatory rheometers*. Germany: Vincentz network GmbH & Co. KG.

Received: Oct. 04, 2022

Revised: Feb. 13, 2023

Accepted: Feb. 14, 2023

Supplementary Information

Supplementary material accompanies this paper.

Table S1. Variables (coded and decoded) studied for optimization of the ultrasonic treatment used for the gum solutions.

Table S2. ANOVA for the response variable η (dL/g).

This material is available as part of the online article from <https://doi.org/10.1590/0104-1428.20220090>